energy&fuels

Article

pubs.acs.org/EF

Laser-Based Mass Spectrometric Assessment of Asphaltene Molecular Weight, Molecular Architecture, and Nanoaggregate Number

Andrew E. Pomerantz,*[,†] Qinghao Wu,[‡] Oliver C. Mullins,[†] and Richard N. Zare[‡]

[†]Schlumberger-Doll Research, Cambridge, Massachusetts 02139, United States

[‡]Department of Chemistry, Stanford University, Stanford, California 94350, United States

ABSTRACT: Unbiased analysis of asphaltene molecules by mass spectrometry requires that the three fundamental steps in mass spectrometry-volatilization, ionization, and mass analysis-are performed reliably and with nearly equivalent efficiency for nearly all of the diverse components in asphaltenes. Here, we examine these three processes and the overall analysis mechanism in two forms of laser-based mass spectrometry: laser desorption laser ionization mass spectrometry (L^2MS) and surface-assisted laser desorption/ionization mass spectrometry (SALDI). In L^2MS, volatilization occurs by laser desorption, which is a thermal process not selective for any particular molecular configuration; ionization occurs by single-photon ionization, which is a soft and universal method applicable to virtually all organic molecules and aggregates; and mass analysis occurs by time-of-flight mass spectrometry, which has a nearly constant sensitivity across a broad mass range. These factors suggest that L^2MS should analyze asphaltenes with almost no bias, and L^2MS measurements of model compounds and asphaltenes provide direct experimental evidence that fragmentation and multiple charging are minimized, while nearly all components of asphaltenes are detected as disaggregated molecules with nearly equivalent sensitivity. These experiments make L^2MS perhaps the most thoroughly studied mass spectrometric method for measuring asphaltene molecules, and the results indicate that L^2MS provides essentially unbiased detection of nearly all of the components in asphaltenes. Similarly, SALDI is demonstrated to be a complementary technique, in which asphaltenes are detected in the form of nanoaggregates. These observations add credibility to conclusions from L^2MS and SALDI that petroleum asphaltenes typically have an average molecular weight in the range of 600−700 Da with an upper mass limit near 1500 Da, asphaltenes are dominated by the island geometry, asphaltenes form stable nanoaggregates containing approximately seven molecules, and asphaltenes of different mass are not separated in a reservoir by gravitational segregation. These results provide a stringent test and confirmation of many components of the Yen−Mullins model, and they support the growing use of the Flory−Huggins−Zuo equation in the oilfield.

INTRODUCTION

Accurate measurement of the chemical composition of asphaltenes is a relevant and long-standing challenge.[1−3] In addition to the flow assurance and refining issues that have occupied asphaltene scientists for many years, asphaltenes are being studied with increasing effort to understand reservoir architecture. In particular, reservoir connectivity is being assessed via analysis of asphaltene gradients[4−6] using the Flory−Huggins−Zuo equation of state,[7−9] which is based on the Yen−Mullins model[10,11] of the molecular and aggregate structure of asphaltenes and enabled by downhole fluid analysis.[12] Continued study of asphaltene chemistry is required to take full advantage of this and other methods of reservoir characterization.

Mass spectrometry has emerged as a powerful tool for studying asphaltenes, owing in part to the diverse methods of detection and quantities measurable under the umbrella of mass spectrometry. In addition to measurements of molecular weight,[3,13−25] mass spectrometry is used to measure other properties of asphaltenes, such as aggregate weight,[18,19,26−28] molecular architecture,[29−32] and elemental composition.[33−35] Although these different methods involve significantly different procedures, several processes are involved in essentially every form of mass spectrometry: the sample must be volatilized, ionized, and then detected.[36] These steps are particularly challenging for asphaltenes, because they require volatilizing molecules that are inherently non-volatile and ionizing molecules that are naturally uncharged. To analyze representative molecules, the volatilization mechanism must be strong enough to break non-covalent bonds holding aggregates together while simultaneously not being excessively strong such that covalent bonds holding molecules together are broken. Similarly, the ionization mechanism must be strong enough to add/remove a charge while simultaneously not being excessively strong such that multiple charges are added/removed. Finally, the mass analyzer must separate ions of different mass sufficiently to resolve them but not so much that they fall outside the observable window. Moreover, these processes must all operate with nearly the same efficiency for all of the distinct components in the complex mixture that is asphaltenes.

Of the many volatilization/ionization methods that have been applied to asphaltenes, several can fail to meet these

Special Issue: 15th International Conference on Petroleum Phase Behavior and Fouling

Received: September 15, 2014
Revised: January 20, 2015
Published: March 11, 2015

DOI: 10.1021/ef5020764
Energy Fuels 2015, 29, 2833−2842

requirements. For example, under certain conditions, the noncovalent forces binding asphaltene aggregates are not broken by laser desorption/ionization[19,21,26,37] or atmospheric pressure ionization techniques.[38] It has been suggested that similar difficulties may be present in other laser-based ionization schemes.[38] Here, we present a series of experiments testing the extent to which all of these requirements are met by two laser-based analyses: surface-assisted laser desorption/ionization mass spectrometry (SALDI–MS), in which a single laser pulse desorbs and ionizes asphaltenes from an activated surface, and laser desorption laser ionization mass spectrometry (L^2MS), in which two spatially and temporally separated lasers desorb and then ionize asphaltenes.

L^2MS has been used many times to measure the composition of asphaltenes.[21,22,26,27,29,30,39,40] Initial asphaltene L^2MS experiments were motivated by the observation that asphaltene molecular-weight distributions measured by single-laser techniques including laser desorption/ionization (LDI) mass spectrometry were inconsistent, with large variations in the observed molecular weight with variations in instrumental operating parameters.[19,37] Unlike LDI, asphaltene molecular-weight distributions measured with L^2MS were found to be insensitive to variations in operating parameters, such as the laser pulse energies, time delay between laser pulses, and sample concentration on the surface over wide ranges.[21,22] Later L^2MS experiments studied molecular architecture in asphaltenes based on the observation that model compounds with archipelago geometry could be fragmented under conditions where model compounds with island geometry could not. Asphaltenes were found not to fragment under those same conditions, suggesting that asphaltenes are dominated by the so-called "island geometry" containing a single aromatic core.[29,30,39] Additional L^2MS measurements of asphaltenes from various locations in a reservoir with a large gradient in the asphaltene content driven by gravitational segregation found nearly identical molecular-weight distributions, suggesting that gravitational segregation does not separate asphaltenes of different molecular weight.[40]

SALDI measurements have been performed more recently on asphaltenes. SALDI measurements of several model compounds show a signal from aggregate structures not observed in L^2MS.[27] SALDI measurements of asphaltenes show a signal from aggregates at a mass of approximately 7 times larger than the mass of asphaltene molecules found in L^2MS, and these signals have been assigned to asphaltene nanoaggregates.[28] Additionally, SALDI measurements have been performed on the same asphaltenes from the gravitationally segregated reservoir, and similar nanoaggregate masses were observed, suggesting that gravitational segregation does not separate asphaltenes of different nanoaggregate weight.[40,41]

Here, we examine the volatilization, ionization, and detection processes in SALDI and, particularly, L^2MS. The mechanism involved in each process is studied to identify potential sources of bias, and measurements of model compounds and asphaltenes are presented to study the role of fragmentation, aggregation, and sensitivity to different components in this complex mixture. Published results based on SALDI and L^2MS measurements are evaluated on the basis of these results.

EXPERIMENTAL SECTION

L^2MS. L^2MS measurements are performed on dry asphaltene powders. Powders are either deposited directly on a glass or metal platter or transferred in solution, followed by evaporating the solvent. The sample is then inserted into a high vacuum chamber through an interlock and held in the vacuum chamber for approximately 15 min to allow for any residual solvent to evaporate. The dry asphaltenes are irradiated with approximately 5 mJ of 10.6 μm infrared (IR) radiation from a CO_2 laser focused to a spot approximately 50 μm in diameter. That IR pulse causes rapid heating of the analyte, approximately 10^8 K/s, and thermal desorption into the vacuum.[42] Because the IR photon energy is nearly 2 orders of magnitude below the ionization potential of asphaltenes, the IR pulse desorbs neutral molecules without ionization. Following a period of approximately 25 μs, in which the neutrals expand into the vacuum, the plume is irradiated by a second laser pulse, which ionizes the desorbed asphaltenes. This second pulse is typically either a 266 nm pulse from a frequency quadrupled Nd:YAG laser, which ionizes asphaltenes via 1 + 1 resonance-enhanced multiphoton ionization (REMPI), or a 157 nm pulse from a F_2 excimer laser, which ionizes asphaltenes via single photon ionization (SPI). The laser power densities are on the order of 10^6 W/cm^2.

The REMPI process is selective for aromatic molecules with ionization potential below the two-photon energy of 9.3 eV,[22] whereas the SPI process is nearly universal for molecules with ionization potential below the single-photon energy of 7.9 eV.[43] In either case, ions are formed under nearly collision-free vacuum conditions. Positive ions are then mass-analyzed by a home-built linear time-of-flight (TOF) mass analyzer operating under Wiley–McLaren conditions[44] with a mass resolution of approximately 1 mass unit at m/z 300. Measurements are typically averaged over many laser shots, with the sample translated between shots to expose a fresh surface to laser desorption. L^2MS has been used to study a wide variety of samples containing organic mixtures, including interplanetary dust,[45] meteorites,[46,47] comets,[48,49] antibiotics,[50] biofilms,[51,52] ancient terrestrial rocks,[53] sediments,[54,55] soils,[56] agricultural samples,[57] polymers,[58] natural water samples,[59] metabolites,[60] and asphaltenes,[21,22,26,28–30,39] and the method has been proposed for *in situ* analysis of organics on planetary missions.[61] Figure 1 shows a photograph of the home-built L^2MS instrument.

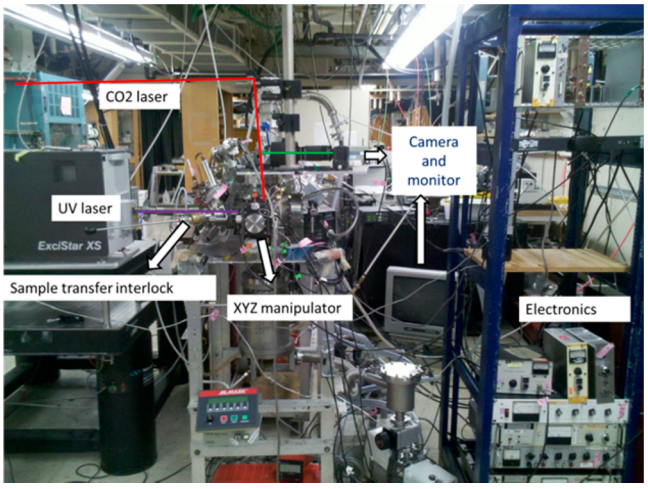

Figure 1. Photograph of the home-built L^2MS instrument, indicating key components. The vacuum chamber in the center of the photograph houses the time-of-flight mass analyzer, and the desorption and ionization laser pulses enter the chamber through windows.

SALDI–MS. SALDI–MS measurements are also performed on dry asphaltene powders under vacuum. The powders are placed on silicon oxide surfaces, which may assist with the desorption/ionization process. The asphaltenes are irradiated with approximately 5 μJ of 337 nm ultraviolet (UV) radiation from a nitrogen laser. This single laser pulse simultaneously desorbs and ionizes the asphaltenes. Positive ions are then mass-analyzed by a TOF mass analyzer (PCS4000, Bio-Rad

DOI: 10.1021/ef5020764
Energy Fuels 2015, 29, 2833–2842

Laboratories). SALDI−MS has been used to study small molecules,[62] peptides and proteins,[63,64] biomolecules,[65] polymers,[66] and asphaltenes.[27,28,40,41]

RESULTS

Accurate mass spectral analysis of asphaltene molecules requires unbiased performance of each of the three fundamental steps in mass spectrometry: volatilization, ionization, and mass analysis. Here, we present mechanistic considerations examining potential sources of bias in each process as applied in L^2MS. Then, we present experimental results examining the role of multiple charging, fragmentation, aggregation, and representative detection of mixtures in L^2MS and SALDI−MS.

Volatilization in L^2MS. Volatilization in L^2MS is achieved by laser desorption. A sample of dry asphaltene powder resting on a glass or metal surface is struck with a 10.6 μm IR pulse from a CO_2 laser. Measurement of the vibrational temperatures of desorbed standards indicates that the desorption mechanism is primarily thermal and involves heating the sample at approximately 10^8 K/s.[42] The rapid heating rate suppresses thermal decomposition of labile molecules. Molecules are desorbed as neutrals, in part because the photon energy (0.1 eV) is 2 orders of magnitude below the ionization potential of asphaltenes.

Accurate measurement of asphaltene molecules by L^2MS requires that essentially all components of asphaltenes are desorbed with equal probability. The thermal desorption mechanism is not selective toward any particular type of molecule, suggesting that laser desorption should not be biased. Additionally, laser desorption has been shown to volatilize molecules heavier than 10 000 Da with no matrix[67] and heavier than 1 000 000 Da with a matrix,[68] much heavier than the reported upper limit of asphaltene molecular weight,[9,10] further suggesting that the desorption in L^2MS should be unbiased. Figure 2 shows asphaltenes deposited on a glass sample platter after L^2MS analysis. The areas covered by asphaltenes are black, while the areas with no asphaltenes appear white. During the L^2MS measurement, the sample was moved diagonally, and the white diagonal lines cutting through the black asphaltene area demonstrate that all or nearly all of the asphaltenes are desorbed from the area where the desorption laser pulse struck the sample. These considerations suggest that essentially all components of asphaltenes are desorbed with equal probability in L^2MS.

Figure 2. Photograph of the asphaltene sample platter after L^2MS measurement. The laser desorption process desorbs essentially all asphaltenes from the area where the laser strikes the sample (white diagonal lines).

Ionization in L^2MS. Ionization in L^2MS is achieved by laser photoionization. The photoionization can be achieved by either two-photon (REMPI) or single-photon (SPI) processes, although SPI is more common. SPI from a F_2 excimer laser involves non-resonant absorption of a 7.9 eV photon, moving the molecule from its ground state to the ionization continuum. REMPI from the fourth harmonic of a Nd:YAG laser involves resonant absorption of two 4.7 eV photons, moving the molecule from its ground state through a real or virtual molecular orbital with sufficient lifetime to the ionization continuum.

Accurate measurement of asphaltene molecules by L^2MS requires that essentially all components of asphaltenes are ionized with nearly equal probability. SPI is the preferred ionization technique because it is considered to be a universal ionization method for organic molecules.[43] One reason that SPI appears to be a universal soft ionization scheme is that the transitions involved are non-resonant; therefore, the probability of ionizing a molecule by SPI is independent of the configuration of the bound molecular orbitals, which can vary greatly between molecules of different compositions. Consistent with its designation as a universal detector, SPI has been used to ionize a diverse set of organic compounds, including fuels,[43] combustion/incineration products,[69] pyrolysis products,[70] foodstuffs,[71] cigarette smoke,[72] metabolites,[60] peptides,[52] pharmaceuticals,[73] high mass species,[68,74] and noncovalently bound aggregates.[75−78]

One potential source of bias in laser ionization is that the technique can ionize only components whose ionization potentials fall below a threshold. That threshold is 7.9 eV in SPI (the single-photon energy) and 9.3 eV in REMPI (the two-photon energy), with the lasers used here. The ionization potential of aromatic molecules with mass >100 Da, which likely encompasses nearly all asphaltenes, is below those thresholds,[43] suggesting that any bias should be small. Additionally, SPI has been shown to ionize large molecules with mass above 10 000 Da, further suggesting that bias toward any particular weight range should be small.[68] The requirement that analytes must have a real or virtual molecular orbital near 4.7 eV to be ionized by this REMPI process potentially induces bias because primarily aromatic molecules meet that requirement, but that bias is again likely to be small because asphaltenes contain approximately 50% aromatic carbon[79] and nearly all asphaltenes are expected to contain at least one aromatic ring,[32] consistent with their color.[80] As a result, asphaltene molecular-weight distributions measured with REMPI and SPI generally agree.[22,30] These considerations suggest that that essentially all components of asphaltenes are ionized with nearly equal probability in L^2MS.

Mass Analysis in L^2MS. Mass analysis in L^2MS is achieved by time-of-flight mass spectrometry (TOF-MS). In TOF-MS, the volatized positive ions created by the two laser pulses are accelerated by a static electric field toward a multichannel plate detector. Their velocity and, therefore, arrival time at the detector depend upon their mass to charge ratio. Assuming the ions are singly charged, the detector signal as a function of the

DOI: 10.1021/ef5020764
Energy Fuels 2015, 29, 2833−2842

arrival time can be converted into a molecular-weight distribution.

Accurate measurement of asphaltene molecules by L^{2}MS requires that essentially all asphaltene ions are detected with equal probability. In comparison to other mass analyzers used for asphaltene analysis, TOF-MS has relatively modest mass resolution and mass accuracy.[36,39] However, TOF-MS has a theoretically unlimited mass range and detects components with nearly equal sensitivity over a large range.[36] As a result, TOF-MS is preferred for samples potentially containing molecules of very large and widely ranging mass.[67,68,81] The use of TOF mass analysis suggests that that essentially all components of asphaltene ions are detected with equal probability in L^{2}MS.

Fragmentation and Multiple Charging in L^{2}MS. Fragmentation and multiple charging of molecules can lead to erroneously low-molecular-weight distributions if fragments or multiply charged ions are assigned as singly charged parent ions. In L^{2}MS, the photon energy provided to ionize the asphaltenes is approximately 1−2 eV above the ionization potential. The leftover energy after ionization is less than the energy required to break a covalent bond (typically 5 eV) or remove a second electron (typically more than 10 eV). Fragmentation and multiple charging, therefore, require absorption of a second photon, and the probability of that second absorption is low as long as the laser power density is held low. As a result, single-photon ionization is considered both a universal and soft ionization technique when the laser power density is low and the photon energy is only slightly greater than the ionization potential.[43] Figure 3 shows SALDI, REMPI−L^{2}MS, and SPI−L^{2}MS spectra of L-tryptophan (ionization potential, 7.2 eV;[82] molecular weight, 204 Da) and caffeic acid (ionization potential, 7.8 eV;[83] molecular weight, 180 Da), two molecules with a strong propensity to fragment in some ionization processes.[27] Similarly, Figure 4 shows SALDI and SPI−L^{2}MS spectra of coronene (ionization potential, 7.3 eV; molecular weight, 300 Da). Several peaks at mass below the parent ion are observed in SALDI, most of which are assigned as fragments. REMPI−L^{2}MS, which has a two-photon energy higher than the single-photon energy in SPI−L^{2}MS and which requires a somewhat higher laser pulse energy than SPI−L^{2}MS to drive the resonant two-photon absorption, also leads to fragmentation. In SPI−L^{2}MS, fragmentation and multiple charging are nearly eliminated; on average for these three molecules, 90% of the total SPI−L^{2}MS signal corresponds to parent ion (86% for L-tryptophan, 86% for caffeic acid, and 98% for coronene), with the remaining 10% coming from fragmented and/or multiply charged species. These considerations suggest that that both fragmentation and multiple charging are rare in SPI−L^{2}MS.

Aggregation in L^{2}MS. Aggregation of ions and molecules can lead to erroneously high-molecular-weight distributions if non-covalently bound aggregates are assigned as molecules or to biased molecular-weight distributions if different components of varying propensity to aggregate are detected with varying efficiency. Aggregation is common in some forms of laser-based mass spectrometry, such as laser desorption/ionization[19,37] or SALDI.[27,28,40] The SPI ionization scheme is commonly used to detect non-covalently bound aggregates,[75−78] suggesting that asphaltene aggregates should be observed in SPI−L^{2}MS if the asphaltenes are in an aggregated state at the time of ionization. One important force binding non-covalent aggregates in mass spectrometric analyses is

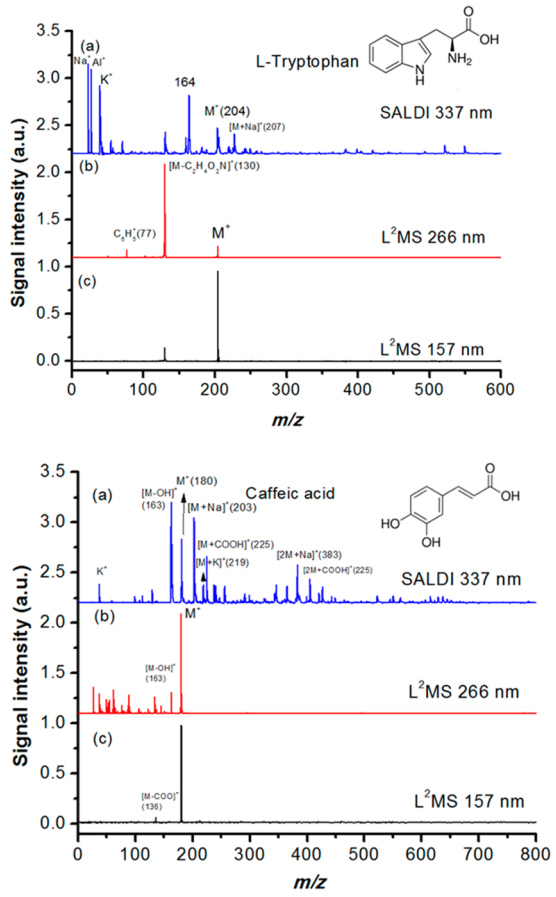

Figure 3. SALDI, REMPI−L^{2}MS, and SPI−L^{2}MS spectra of L-tryptophan and caffeic acid, showing that fragmentation, multiple charging, and aggregation are suppressed in SPI−L^{2}MS.[27]

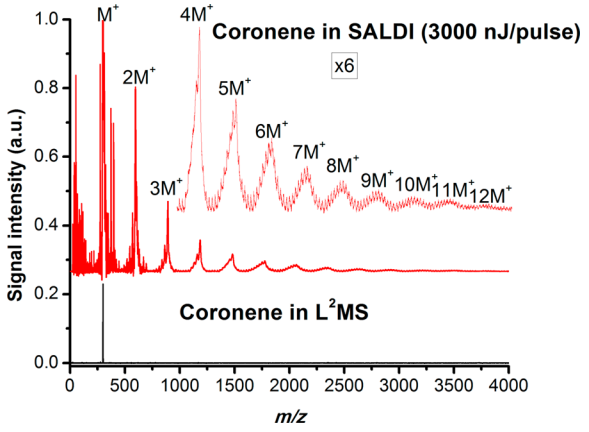

Figure 4. SALDI (red) and SPI−L^{2}MS (black) spectra of coronene. Coronene is detected in the aggregated form in SALDI and in the isolated molecular form in SPI−L^{2}MS.[28]

electrostatic attraction between an ionized molecule and an induced dipole in a nearby neutral molecule (ion-induced dipole attraction).[21] Although this force is significant in many laser-based mass spectrometric processes, it is nearly eliminated in L^{2}MS. In L^{2}MS, the desorbed plume of neutral molecules expands into the vacuum prior to ionization, in the time between the desorption and ionization laser pulses. Because the molecules are not ionized during the expansion, no ion-induced dipole force exists at that time. By the time of ionization, the

DOI: 10.1021/ef5020764
Energy Fuels 2015, 29, 2833−2842

molecules have dispersed into the vacuum until they are too far from each other to exert an ion-induced dipole force, such that this force cannot cause aggregation in L^{2}MS. As a result, signals from products of ion−molecule reactions, which can be observed in laser desorption/ionization experiments, are not observed in L^{2}MS.[84] Aggregation in L^{2}MS may be further suppressed by interactions with the IR pulse[22,85,86] or the photoionization process.[22,87]

Figure 4 presents SALDI and SPI−L^{2}MS spectra of coronene (molecular weight, 300 Da).[40] Coronene is more strongly aggregating than asphaltenes; it is a solid that is only sparingly soluble in toluene, because the large aromatic surface allows for strong π-stacking interactions without disruption from aliphatic chains.[88] Aggregates containing up to 12 molecules are observed in the SALDI spectrum, perhaps expected because of the strong aggregation. In the SPI−L^{2}MS spectrum, no aggregate signal is observed, demonstrating that the SPI−L^{2}MS process suppresses aggregation even in strongly aggregating molecules. These considerations suggest that asphaltenes and other molecules prone to aggregation are detected as isolated molecules in L^{2}MS.

Aggregation in SALDI. Mass spectrometry is an inherently destructive measurement, because either adding an electric charge to or removing an electric charge from the analyte is required. Many ionization techniques further destroy the analyte, with methods such as inductively coupled plasma ionization typically breaking all covalent and non-covalent bonds, thereby detecting individual elements.[36] In laser-based mass spectrometry, covalent and non-covalent bonds can readily be broken by use of high laser pulse energy.[29,30] As described above, in L^{2}MS, covalent bonds can be preserved by the use of SPI at low laser pulse energy, but breaking non-covalent bonds is unavoidable. SALDI is a less destructive ionization technique than SPI−L^{2}MS, and in SALDI, some non-covalent bonds can be preserved or formed at low laser pulse energy. One explanation for the observation of non-covalently bound aggregates in SALDI but not in L^{2}MS is that the ion-induced dipole forces absent in L^{2}MS are present in SALDI. These forces occur in SALDI because the ionization occurs simultaneously with the desorption, at a time where the pressure is still relatively high and the intermolecular distance is relatively short. Preservation or formation of asphaltene aggregates has been demonstrated in other laser-based mass spectrometry techniques, where desorption and ionization occur simultaneously.[18,19,26,37]

Figure 5 shows the SALDI mass spectra of a petroleum asphaltene recorded over a range of laser pulse energies.[28] The most intense high mass signal is detected primarily at low laser pulse energy, only slightly above the threshold pulse energy required for observing any signal. That signal occurs at mass approximately 7 times larger than the mass of asphaltene molecules observed in SPI−L^{2}MS or REMPI−L^{2}MS, leading to its assignment as asphaltene nanoaggregates.[28] At increasing laser pulse energy, the nanoaggregate is broken up into smaller multimers, as expected because of the weak binding of asphaltene nanoaggregates.[89] These results suggest that asphaltenes can be detected as nanoaggregates in SALDI measurements at low laser pulse energy.

Detecting Complex Mixtures in L^{2}MS. Unbiased measurement of the average properties of complex mixtures presents the additional difficulty that all components of the mixture must be detected with comparable efficiency. Overcoming this challenge can be difficult with ionization

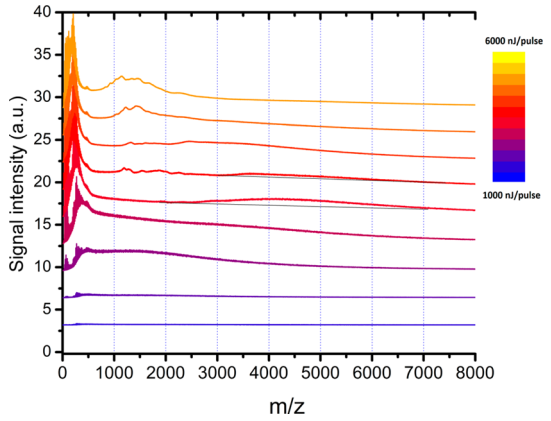

Figure 5. SALDI spectra of asphaltenes at varying laser pulse energies. Raw spectra are shown, with black lines indicating exponentially decreasing baseline as described previously.[28] At low laser pulse energies (slightly above the threshold for observing signal), some asphaltenes are detected as nanoaggregates, while at higher laser pulse energies, the nanoaggregates are broken up into small multimers.

techniques that sensitively depend upon the properties of the analytes, such as atmospheric pressure ionization techniques, where ionization generally involves ion−molecule reactions, whose rate constants can vary over large ranges.[36] As described above, in SPI−L^{2}MS, the volatilization, ionization, and detection processes are relatively insensitive to the composition of the analyte and are expected to occur with similar efficiency for all components of asphaltenes. As a result, it is anticipated that SPI−L^{2}MS will make an almost unbiased measurement of asphaltenes. This hypothesis can be tested by performing SPI−L^{2}MS measurements on mixtures.

Figure 6 presents the SPI−L^{2}MS spectrum of a simple equimolar mixture of five model compounds, including

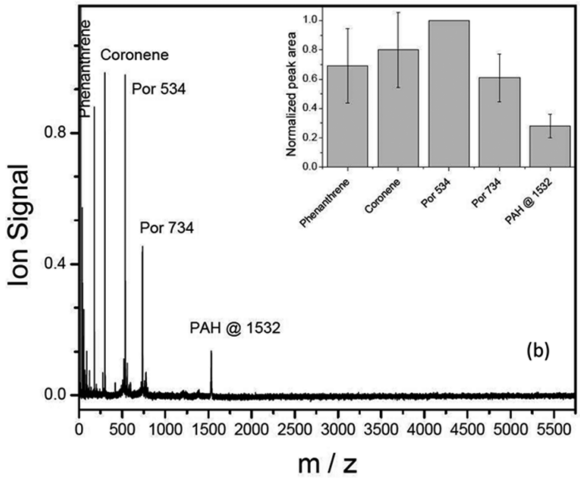

Figure 6. SPI−L^{2}MS spectrum of an equimolar mixture of phenanthrene, coronene, 2,3,7,8,12,13,17,18-octaethyl-21*H*,23*H*-porphine (Por 534), 5,10,15,20-tetrakis(4-methoxyphenyl)-21*H*,23*H*-porphine (Por 734), and alkylated peri-condensed hexabenzocoronene[91] (PAH at 1532). The *y* axis is in arbitrary units. The main figure shows the raw data, while the inset shows the peak areas normalized to Por 534. Peak heights decrease systematically at higher mass because peak width increases as a result of diminished mass resolution at higher mass. Integrating the peak areas shows that SPI−L^{2}MS detects these compounds with equal sensitivity within a factor of 3.[39]

DOI: 10.1021/ef5020764
Energy Fuels 2015, 29, 2833−2842

polycyclic aromatic hydrocarbons (PAHs), alkylated PAHs, and porphyrins spanning a mass range of 178−1532 Da.[39] As expected, this spectrum of five components contains principally five peaks, with little signal observed from fragmentation products and essentially no signal observed from aggregated species. Additionally, the signal strength from these five diverse components is equivalent within a factor of 3, with no correlation between SPI−L^{2}MS relative sensitivity and molecular weight. The peak height in the raw SPI−L^{2}MS data decreases with increasing mass because the mass resolution of TOF-MS decreases with increasing mass, resulting in peaks that are shorter but wider at higher mass. When those peaks are integrated, it is found that the peak areas are nearly equivalent, as shown in the inset of the figure. The sensitivities are more similar than those found in other techniques, such as electrospray ionization, which has large variation in sensitivity, for example, between polar and nonpolar analytes.[90] In particular, the sensitivity is not significantly decreased for alkylated peri-condensed hexabenzocoronene[91] (PAH at 1532), which is nonpolar, has higher molecular mass than average asphaltenes, and has lower aromaticity than average asphaltenes. In addition to the nearly equivalent detection sensitivities shown here for PAHs, alkylated PAHs, and porphyrins, similar results have been observed for N-, S-, and O-substituted PAHs.[39]

Figure 7 presents the SPI−L^{2}MS spectrum of a complex mixture of asphaltenes spiked with one porphyrin.[39] Integrating the peak area and normalizing by the concentration show that the porphyrin and asphaltenes are detected with comparable efficiency again within a factor of 3. While consideration of the volatilization, ionization, and detection mechanisms in SPI−L^{2}MS suggests that different components of asphaltenes should be detected with similar efficiency, these data strongly suggest that different components of asphaltenes are detected with similar efficiency in SPI−L^{2}MS.

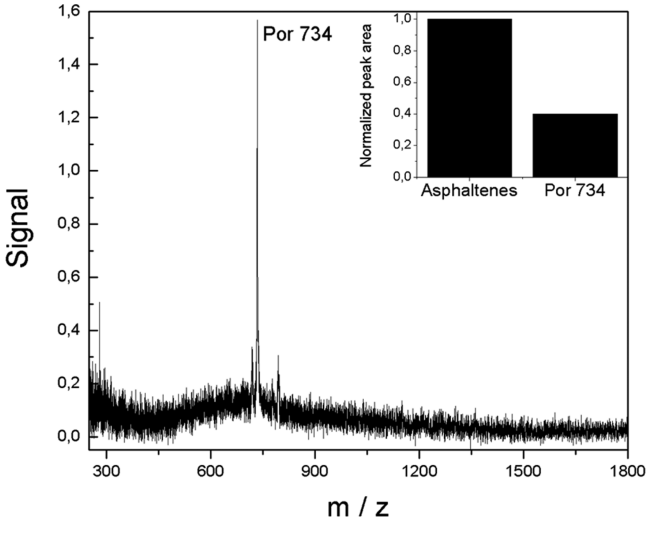

Figure 7. SPI−L^{2}MS spectrum of a petroleum asphaltene mixed with 5,10,15,20-tetrakis(4-methoxyphenyl)-21*H*,23*H*-porphine (Por 734). The *y* axis is in arbitrary units. The main figure shows the raw data, while the inset shows the peak areas normalized to the sample concentration (the sample was mixed in a molar ratio of 2:1 asphaltene/porphyrin). SPI−L^{2}MS detects asphaltenes and this model compound with equal sensitivity within a factor of 3.[39]

DISCUSSION

L^{2}MS has been used previously to examine asphaltene molecular weight[21,22,26,28,39] and molecular architecture,[29,30] and SALDI has been used to examine asphaltene nanoaggregate weight.[27,28] Both techniques have been used to examine the heterogeneity of asphaltenes from different locations in a reservoir.[40] The evidence presented here that SPI−L^{2}MS detects nearly all components of asphaltenes (including PAHs, alkylated PAHs, heteroatom-substituted PAHs, and porphyrins) with nearly equivalent sensitivity and with minimal influence of multiple charging, fragmentation, or aggregation allows for these results to be interpreted with increased confidence.

Molecular-weight measurements of petroleum asphaltenes measured by SPI−L^{2}MS and REMPI−L^{2}MS generally agree, showing average molecular weights near 600−700 Da and upper mass cutoffs near 1500 Da. Petroleum asphaltenes from various reservoirs have only subtle differences in molecular weight, while coal-derived asphaltenes are approximately half the mass of petroleum asphaltenes.[22,28] A low mass signal is observed in some asphaltene samples and is assigned to fragments, motivating further efforts to suppress residual fragmentation to below the 10% level obtained currently.[28,40] The results presented here showing the ability of these analyses to detect a wide range of masses with comparable sensitivity adds confidence to the average and upper mass limit estimates. The comparable results obtained with the two ionization schemes suggest that each is ionizing asphaltenes representatively, and the measured molecular weights agree with other measurements based on different physics, such as diffusion constant measurements,[9−11] further strengthening the conclusions on the asphaltene molecular-weight distribution.

Molecular architecture measurements of asphaltenes by L^{2}MS investigate the abundance of molecules with island geometries and archipelago geometries. A series of 10 model compounds with archipelago geometries and 13 model compounds with island geometries were studied with REMPI−L^{2}MS.[30] All model compounds with archipelago geometry were found to fragment more extensively with increasing laser pulse energy. Over that same laser pulse energy range, all model compounds with island geometry did not fragment. Similar to the island structure model compounds, asphaltenes were also found not to fragment, suggesting that asphaltenes are dominated by the island architecture. The results presented here showing that L^{2}MS detects most components of asphaltenes with nearly the same sensitivity suggest that these model compound studies with L^{2}MS are an effective approach for characterizing asphaltenes, although repeated studies on additional model compounds of a more diverse chemistry could further increase confidence in the conclusions.

SALDI measurements at a low laser pulse energy observed a signal at a mass of approximately 7 times the asphaltene molecular mass as measured by L^{2}MS.[28] The results presented here showing that SALDI is a more gentle technique than L^{2}MS, able to preserve or form non-covalently bound aggregates that are disaggregated in L^{2}MS, suggest that this signal corresponds to aggregated asphaltenes. This signal appears at a size larger than that observed for asphaltene molecules but similar to that observed for asphaltene nanoaggregates.[9−11] It appears that the challenge in laser-based mass spectrometry is not breaking up aggregates but

DOI: 10.1021/ef5020764
Energy Fuels 2015, 29, 2833−2842

preserving them. Asphaltene nanoaggregates are formed at moderate concentrations in toluene, as measured by techniques, such as nuclear magnetic resonance (NMR),[92] high-Q ultrasonics,[93] and mass spectrometry.[38] Thermodynamic analysis of this concentration suggests that asphaltene nanoaggregates are weakly bound, potentially explaining the difficultly in preserving them.[89]

SPI–L^{2}MS and SALDI have been used to study the composition of asphaltenes from different locations in a reservoir in which the asphaltene concentration in the crude varies by an order of magnitude, driven primarily by gravitational segregation.[40] It was found that both the asphaltene molecular mass and nanoaggregate mass are constant across the reservoir. The results presented here showing that SPI–L^{2}MS and SALDI make representative measurements of asphaltene composition strengthen the conclusion that gravitational segregation creates gradients in the concentration of asphaltenes but not in the composition of those asphaltenes. These conclusions are supported by measurements of the sulfur chemistry of these same samples.[41,94]

This work provides a stringent test and confirmation of the Yen–Mullins model.[10,11] Many other recent studies also confirm this model, including NMR measurements,[95,96] interfacial tension measurements,[97,98] combined small-angle neutron scattering and small-angle X-ray scattering,[99] combined direct current (DC) conductivity and centrifugation studies,[89] and field studies.[4−6,8]

CONCLUSION

Mass spectrometric analysis of complex mixtures involves several steps, each of which must be performed reliably to draw representative conclusions. These steps include volatilization, which must be strong enough to break non-covalent bonds but not so strong as to break covalent bonds; ionization, which must be strong enough to remove an electron but not so strong as to remove multiple electrons; and mass analysis, which must separate ions of different mass sufficiently to resolve them but not so much that they fall outside the observable window. Additionally, each of these processes must have nearly equal efficiency for nearly all of the components in a mixture.

Several techniques cannot meet these varied challenges simultaneously. For example, atmospheric pressure ionization techniques coupled to Fourier transform ion cyclotron resonance (FT-ICR) mass analyzers are relatively insensitive to a fraction of asphaltene molecules with strong propensity to aggregate.[38] Analysis of the mass defects measured by L^{2}MS suggests that L^{2}MS may suffer from the same challenges.[38] However, the mass resolution and mass accuracy of TOF-MS used in L^{2}MS is inherently low (orders of magnitude below typical values for modern FT-ICR instruments), preventing the L^{2}MS measurement from being calibrated with the accuracy required to draw meaningful conclusions from the measured mass defect.[36]

A comprehensive investigation of the performance of L^{2}MS is presented here. Consideration of the volatilization, ionization, and detection mechanisms in L^{2}MS suggests that there should be little bias in the measurement of asphaltenes. Volatilization occurs by laser desorption, which involves a thermal mechanism that is not selective toward any particular molecular structure and has been demonstrated to be effective for molecules with mass much larger than the upper limit of asphaltenes.[67] Ionization occurs under vacuum conditions by SPI, which is a universal and soft ionization technique known to be effective for a variety of molecules and aggregates.[43] Mass analysis occurs by TOF-MS, which offers nearly constant sensitivity across a mass range that is theoretically unlimited and experimentally demonstrated to extend over a large range extending to mass much larger than the upper limit of asphaltenes. Direct measurement of asphaltenes and model compounds provide experimental evidence that bias in L^{2}MS is small. Both fragile compounds and strongly aggregating compounds are detected by SPI–L^{2}MS, with 90% of the signal corresponding to singly charged parent ions, 10% corresponding to fragmented or multiply charged species, and nearly 0% corresponding to aggregates. Measurements of simple and complex mixtures suggest that the different components of asphaltenes are detected with nearly the same sensitivity in SPI–L^{2}MS. This set of experiments makes L^{2}MS perhaps the most thoroughly studied mass spectrometric method for measuring asphaltene molecules, and the results suggest that L^{2}MS provides an unbiased measurement of nearly all of the components in asphaltenes. The observations add credibility to conclusions from L^{2}MS and SALDI that petroleum asphaltenes typically have an average molecular weight in the range of 600–700 Da with an upper mass limit near 1500 Da, asphaltenes are dominated by the island geometry, asphaltenes form stable nanoaggregates containing approximately seven molecules, and asphaltenes of different mass are not separated in a reservoir by gravitational segregation.

AUTHOR INFORMATION

Corresponding Author

*E-mail: apomerantz@slb.com.

Notes

The authors declare no competing financial interest.

REFERENCES

(1) Marshall, A. G.; Rodgers, R. P. Petroleomics: The next grand challenge for chemical analysis. *Acc. Chem. Res.* **2004**, *37*, 53–59.

(2) Strausz, O. P.; Safarik, I.; Lown, E. M.; Morales-Izquierdo, A. A critique of asphaltene fluorescence deacy and depolarization-based claims about molecular weight and molecular architecture. *Energy Fuels* **2008**, *22*, 1156–1166.

(3) Mullins, O. C.; Martínez-Haya, B.; Marshall, A. G. Contrasting perspective on asphaltene molecular weight. This comment vs the overview of A. A. Herod, K. D. Bartle, and R. Kandiyoti. *Energy Fuels* **2008**, *22*, 1765–1773.

(4) Betancourt, S. S.; Ventura, G. T.; Pomerantz, A. E.; Viloria, O.; Dubost, F. X.; Zuo, J.; Monson, G.; Bustamante, D.; Purcell, J. M.; Nelson, R. K.; Rodgers, R. P.; Reddy, C. M.; Marshall, A. G.; Mullins, O. C. Nanoaggregates of asphaltenes in a reservoir crude oil and reservoir connectivity. *Energy Fuels* **2009**, *23*, 1178–1188.

(5) Pomerantz, A. E.; Ventura, G. T.; McKenna, A. M.; Cañas, J. A.; Auman, J.; Koerner, K.; Curry, D.; Nelson, R. K.; Reddy, C. M.; Rodgers, R. P.; Marshall, A. G.; Peters, K. E.; Mullins, O. C. Combining biomarker and bulk compositional gradient analysis to assess reservoir connectivity. *Org. Geochem.* **2010**, *41*, 812–821.

(6) Dong, C.; Petro, D.; Pomerantz, A. E.; Nelson, R. K.; Latifzai, A. S.; Nouvelle, X.; Zuo, J. Y.; Reddy, C. M.; Mullins, O. C. New thermodynamic modeling of reservoir crude oil. *Fuel* **2014**, *117*, 839–850.

(7) Freed, D. E.; Mullins, O. C.; Zuo, J. Y. Theoretical treatment of asphaltene gradients in the presence of GOR gradients. *Energy Fuels* **2010**, *24*, 3942–3949.

(8) Zuo, J. Y.; Mullins, O. C.; Freed, D.; Elshahawi, H.; Dong, C.; Seifert, D. J. Advances in the Flory–Huggins–Zuo equation of state

DOI: 10.1021/ef5020764
Energy Fuels 2015, 29, 2833–2842

for asphaltene gradients and formation evaluation. *Energy Fuels* **2013**, *27*, 1722−1735.
(9) Mullins, O. C.; Pomerantz, A. E.; Zuo, J. Y.; Dong, C. Downhole fluid analysis and asphaltene science for petroleum reservoir evaluation. *Annu. Rev. Chem. Biomol. Eng.* **2014**, *5*, 325−345.
(10) Mullins, O. C. The modified Yen model. *Energy Fuels* **2010**, *24*, 2179−2207.
(11) Mullins, O. C.; Sabbah, H.; Eyssautier, J.; Pomerantz, A. E.; Barré, L.; Andrews, A. B.; Ruiz-Morales, Y.; Mostowfi, F.; McFarlane, R.; Goual, L.; Lepkowicz, R.; Cooper, T.; Orbulescu, J.; Leblanc, R. M.; Edwards, J.; Zare, R. N. Advances in asphaltene science and the Yen−Mullins model. *Energy Fuels* **2012**, *26*, 3986−4003.
(12) Mullins, O. C. *The Physics of Reservoir Fluids: Discovery through Downhole Fluid Analysis*; Schlumberger: Sugar Land, TX, 2008; p 184.
(13) Al-Muhareb, E.; Morgan, T. J.; Herod, A. A.; Kandiyoti, R. Characterization of petroleum asphaltenes by size exclusion chromatography, UV-fluorescence and mass spectrometry. *Pet. Sci. Technol.* **2007**, *25*, 81−91.
(14) Acevedo, S.; Gutierrez, L. B.; Negrin, G.; Pereira, J. C.; Mendez, B.; Delolme, F.; Dessalces, G.; Broseta, D. Molecular weight of petroleum asphaltenes: A comparison between mass spectrometry and vapor pressure osmometry. *Energy Fuels* **2005**, *19*, 1548−1560.
(15) Herod, A. A.; Bartle, K. D.; Kandiyoti, R. Characterization of heavy hydrocarbons by chromatographic and mass spectrometric methods: An overview. *Energy Fuels* **2007**, *21*, 2176−2203.
(16) Boduszynski, M. M. Composition of heavy petroleums. 1. Molecular weight, hydrogen defiency, and heteroatom concentration as a function of atmospheric equivalent boiling point up to 1400 °F (760 °C). *Energy Fuels* **1987**, *1*, 2−11.
(17) Qian, K.; Edwards, K. E.; Siskin, M.; Olmstead, W. N.; Mennito, A. S.; Dechert, G. J.; Hoosain, N. E. Desorption and ionization of heavy petroleum molecules and measurements of molecular weight distributions. *Energy Fuels* **2007**, *21*, 1042−1047.
(18) Hortal, A. R.; Hurtado, P.; Martínez-Haya, B.; Mullins, O. C. Molecular weight distributions of coal and petroleum asphaltenes from laser desorption/ionization experiments. *Energy Fuels* **2007**, *21*, 2863−2868.
(19) Hortal, A. R.; Martínez-Haya, B.; Lobato, M. D.; Pedrosa, J. M.; Lago, S. On the determination of molecular weight distributions of asphaltenes and the aggregates in laser desorption ionization experiments. *J. Mass Spectrom.* **2006**, *41*, 960−968.
(20) Cunico, R. L.; Sheu, E. Y.; Mullins, O. C. Molecular weight measurement of UG8 asphaltene using APCI mass spectrometry. *Pet. Sci. Technol.* **2004**, *22*, 787−798.
(21) Pomerantz, A. E.; Hammond, M. R.; Morrow, A. L.; Mullins, O. C.; Zare, R. N. Two-step laser mass spectrometry of asphaltenes. *J. Am. Chem. Soc.* **2008**, *130*, 7216−7217.
(22) Pomerantz, A. E.; Hammond, M. R.; Morrow, A. L.; Mullins, O. C.; Zare, R. N. Asphaltene molecular-mass distribution determined by two-step laser mass spectrometry. *Energy Fuels* **2009**, *23*, 1162−1168.
(23) Sheu, E. Y. Petroleum asphaltene—Properties, characterization, and issues. *Energy Fuels* **2002**, *16*, 74−82.
(24) Strausz, O. P.; Peng, P.; Murgich, J. About the colloidal nature of asphaltenes and the MW of covalent monomeric units. *Energy Fuels* **2002**, *16*, 809−822.
(25) Tanaka, R.; Sato, S.; Takanohashi, T.; Hunt, J. E.; Winans, R. E. Analysis of the molecular weight distribution of petroleum asphaltenes using laser desorption−mass spectrometry. *Energy Fuels* **2004**, *18*, 1405−1413.
(26) Hurtado, P.; Gámez, F.; Martínez-Haya, B. One- and two-step ultraviolet and infrared laser desorption ionization mass spectrometry of asphaltenes. *Energy Fuels* **2010**, *24*, 6067−6073.
(27) Wu, Q.; Pomerantz, A. E.; Mullins, O. C.; Zare, R. N. Minimization of fragmentation and aggregation by laser desorption laser ionization mass spectrometry. *J. Am. Soc. Mass Spectrom.* **2013**, *24*, 1116−1122.
(28) Wu, Q.; Pomerantz, A. E.; Mullins, O. C.; Zare, R. N. Laser-based mass spectrometric determination of aggregation numbers for petroleum- and coal-derived asphaltenes. *Energy Fuels* **2014**, *28*, 475−482.
(29) Sabbah, H.; Morrow, A. L.; Pomerantz, A. E.; Mullins, O. C.; Tan, X.; Gray, M. R.; Azyat, K.; Tykwinski, R. R.; Zare, R. N. Comparing laser desorption/laser ionization mass spectra of asphaltenes and model compounds. *Energy Fuels* **2010**, *24*, 3589−3594.
(30) Sabbah, H.; Morrow, A. L.; Pomerantz, A. E.; Zare, R. N. Evidence for island structures as the dominant architecture of asphaltenes. *Energy Fuels* **2011**, *25*, 1597−1604.
(31) Hurt, M. R.; Borton, D. J.; Choi, H. J.; Kenttämaa, H. I. Comparison of the structures of molecules in coal and petroleum asphaltenes by using mass spectrometry. *Energy Fuels* **2013**, *27*, 3653−3658.
(32) McKenna, A. M.; Marshall, A. G.; Rodgers, R. P. Heavy petroleum composition. 4. Asphaltene compositional space. *Energy Fuels* **2013**, *27*, 1257−1267.
(33) Marshall, A. G.; Rodgers, R. P. Petroleomics: Chemistry of the underworld. *Proc. Natl. Acad. Sci. U. S. A.* **2008**, *105*, 18090−18095.
(34) Pomerantz, A. E.; Mullins, O. C.; Paul, G.; Ruzicka, J.; Sanders, M. Orbitrap mass spectrometry: A proposal for routine analysis of nonvolatile components of petroleum. *Energy Fuels* **2011**, *25*, 3077−3082.
(35) Klitzke, C. F.; Corilo, Y. E.; Siek, K.; Binkley, J.; Patrick, J.; Eberlin, M. N. Petroleomics by ultrahigh-resolution time-of-flight mass spectrometry. *Energy Fuels* **2012**, *26*, 5787−5794.
(36) de Hoffmann, E.; Stroobant, V. *Mass Spectrometry: Principles and Applications*, 3rd ed.; John Wiley & Sons, Ltd.: Chichester, U.K., 2007; p 489.
(37) Martínez-Haya, B.; Hortal, A. R.; Hurtado, P.; Lobato, M. D.; Pedrosa, J. M. Laser desorption/ionization determination of molecular weight distributions of polyaromatic carbonaceous compounds and their aggregates. *J. Mass Spectrom.* **2007**, *42*, 701−713.
(38) McKenna, A. M.; Donald, L. J.; Fitzsimmons, J. E.; Juyal, P.; Spicer, V.; Standing, K. G.; Marshall, A. G.; Rodgers, R. P. Heavy petroleum composition. 3. Asphaltene aggregation. *Energy Fuels* **2013**, *27*, 1246−1256.
(39) Sabbah, H.; Pomerantz, A. E.; Wagner, M.; Müllen, K.; Zare, R. N. Laser desorption single-photon ionization of asphaltenes: Mass range, compound sensitivity, and matrix effects. *Energy Fuels* **2012**, *26*, 3521−3526.
(40) Wu, Q.; Seifert, D. J.; Pomerantz, A. E.; Mullins, O. C.; Zare, R. N. Constant asphaltene molecular and nanoaggregate mass in a gravitationally segregated reservoir. *Energy Fuels* **2014**, *28*, 3010−3015.
(41) Pomerantz, A. E.; Seifert, D. J.; Qureshi, A.; Zeybek, M.; Mullins, O. C. The molecular composition of asphaltenes in a highly compositionally graded column. *Petrophysics* **2013**, *54*, 427−238.
(42) Maechling, C. R.; Clemett, S. J.; Engelke, F.; Zare, R. N. Evidence for thermalization of surface-desorbed molecules at heating rates of 10^8 K/s. *J. Chem. Phys.* **1996**, *104*, 8768−8776.
(43) Hanley, L.; Zimmermann, R. Light and molecular ions: The emergence of vacuum UV single-photon ionization in MS. *Anal. Chem.* **2009**, *81*, 4174−4182.
(44) Wiley, W. C.; McLaren, I. H. Time-of-flight mass spectrometer with improved resolution. *Rev. Sci. Instrum.* **1955**, *26*, 1150.
(45) Clemett, S. J.; Maechling, C. R.; Zare, R. N.; Swan, P. D.; Walker, R. M. Identification of complex aromatic molecules in individual interplanetary dust particles. *Science* **1993**, *262*, 721−725.
(46) Hahn, J. H.; Zenobi, R.; Bada, J. L.; Zare, R. N. Application of two-step laser mass spectrometry to cosmogeochemistry: Direct analysis of meteorites. *Science* **1988**, *239*, 1523−1525.
(47) Clemett, S. J.; Zare, R. N. Microprobe two-step laser mass spectrometry as an analytical tool for meteoric samples. In *Molecules in Astrophysics: Probes and Processes*; van Dishoeck, E. F., Ed.; Kluwer Academic Publishers: Dordrecht, Netherlands, 1997; pp 305−320.
(48) Brownlee, D.; et al. Comet 81P/Wild 2 under a microscope. *Science* **2006**, *314*, 1711−1716.
(49) Sandford, S. A.; et al. Organics captured from comet 81P/Wild 2 by the Stardust spacecraft. *Science* **2006**, *314*, 1720−1724.

DOI: 10.1021/ef5020764
Energy Fuels 2015, 29, 2833−2842

(50) Gasper, G. L.; Carlson, R.; Akhmetov, A.; Moore, J. F.; Hanley, L. Laser desorption 7.87 eV postionization mass spectrometry of antibiotics in *Staphylococcus epidermidis* bacterial biofilms. *Proteomics* **2008**, *8*, 3816−3821.
(51) Akhmetov, A.; Moore, J. F.; Gasper, G. L.; Koin, P. J.; Hanley, L. Laser desorption postionization for imaging MS of biological material. *J. Mass Spectrom.* **2010**, *45*, 137−145.
(52) Edirisinghe, P. D.; Moore, J. F.; Skinner-Nemec, K. A.; Lindberg, C.; Giometti, C. S.; Veryovkin, I. V.; Hunt, J. E.; Pellin, M. J.; Hanley, L. Detection of in situ derivatized peptides in microbial biofilms by laser desorption 7.87 eV postionizaton mass spectrometry. *Anal. Chem.* **2007**, *79*, 508−514.
(53) Mahajan, T. B.; Plows, F. L.; Gillette, J. S.; Zare, R. N.; Logan, G. A. Comparison of microprobe two-step laser desorption/laser ionization mass spectrometry and gas chromatography/mass spectrometry studies of polycyclic aromatic hydrocarbons in ancient terrestrial rocks. *J. Am. Soc. Mass Spectrom.* **2001**, *12*, 989−1001.
(54) Gillette, J. S.; Ghosh, U.; Mahajan, T. B.; Zare, R. N.; Luthy, R. G. Microprobe laser mass spectrometry studies of polycyclic aromatic hydrocarbon distributions on harbor sediments and coals. *Isr. J. Chem.* **2001**, *41*, 105−110.
(55) Ghosh, U.; Gillette, J. S.; Luthy, R. G.; Zare, R. N. Microscale location, characterization, and association of polycyclic aromatic hydrocarbons on harbor sediment particles. *Environ. Sci. Technol.* **2000**, *34*, 1729−1736.
(56) Wang, H.-L.; Hu, Y.-J.; Xing, D. Recent progress of two-step laser desorption/laser ionization mass spectrometry and its application. *Chin. J. Anal. Chem.* **2011**, *39*, 276−282.
(57) Orea, J. M.; Montero, C.; Jimenez, J. B.; Gonzalez Urena, A. Analysis of *trans*-resveratrol by laser desorption coupled with resonant ionization spectrometry. Application to *trans*-resveratrol content in vine leaves and grape skin. *Anal. Chem.* **2001**, *73*, 5921−5929.
(58) Zhan, Q.; Zenobi, R.; Wright, S. J.; Langridge-Smith, P. R. R. Spatially resolved in-situ analysis of polymer additives by two-step laser mass spectrometry. *Macromolecules* **1996**, *29*, 7865−7871.
(59) Bucheli, T. D.; Haefliger, O. P.; Dietiker, R., Jr.; Zenobi, R. Analysis of water contaminants and natural water samples using two-step laser mass spectrometry. *Anal. Chem.* **2000**, *72*, 3671−3677.
(60) Chen, Y.; Sullards, M. C.; Hoang, T. T.; May, S. W.; Orlando, T. M. Analysis of organoselenium and organic acid metabolites by laser desorption single photon ionization mass spectrometry. *Anal. Chem.* **78**, *78*, 8386−8394.
(61) Getty, S. A.; Brinckerhoff, W. B.; Cornish, T.; Ecelberger, S.; Floyd, M. Compact two-step laser time-of-flight mass spectrometer for in situ analyses of aromatic organics on planetary missions. *Rapid Commun. Mass Spectrom.* **2012**, *26*, 2786−2790.
(62) Kailasa, S. K.; Wu, H. F. Interference free detection for small molecules: probing the Mn^{2+}-doped effect and cysteine capped effect on the ZnS nanoparticles for coccidiostats and peptide analysis in SALDI−TOF MS. *Analyst* **2010**, *135*, 1115−1123.
(63) Duan, J.; Linman, M. J.; Chen, C. Y.; Cheng, Q. J. CHCA-modified Au nanoparticles for laser desorption ionization mass spectrometric analysis of peptides. *J. Am. Soc. Mass Spectrom.* **2009**, *20*, 1530−1539.
(64) Chiang, C. H.; Yang, Z.; Lin, Y.-W.; Chen, W.-T.; Lin, H.-J.; Chang, H.-T. Detection of proteins and protein−ligand complexes using HgTe nanostructure matrixes in surface-assisted laser desorption/ionization mass spectrometry. *Anal. Chem.* **2010**, *82*, 4543−4550.
(65) Duan, J.; Linman, M. J.; Cheng, Q. Ultrathin calcinated films on a gold surface for highly effective laser desorption/ionization of biomolecules. *Anal. Chem.* **2010**, *82*, 5088−5094.
(66) Watanabe, T.; Kawasaki, H.; Yonezawa, T.; Arakawa, R. Surface-assisted laser desorption/ionization mass spectrometry (SALDI−MS) of low molecular weight organic compounds and synthetic polymers using zinc oxide (ZnO) nanoparticles. *J. Mass Spectrom.* **2008**, *43*, 1063−1071.
(67) Schriemer, D. C.; Li, L. Detection of high molecular weight narrow polydisperse polymers up to 1.5 million daltons by MALDI mass spectrometry. *Anal. Chem.* **1996**, *68*, 2721−2725.
(68) Schmid, P.; Stohr, F.; Arndt, M.; Tuxen, J.; Mayor, M. Single-photon ionization of organic molecules beyond 10 kDa. *J. Am. Soc. Mass Spectrom.* **2012**, *24*, 602−608.
(69) Kuribayashi, S.; Yamakoshi, H.; Danno, M.; Sakai, S.; Tsuruga, S.; Futami, H.; Morii, S. VUV single-photon ionization ion trap time-of-flight mass spectrometer for on-line, real-time monitoring of chlorinated organic compounds in waste incineration flue gas. *Anal. Chem.* **2005**, *77*, 1007−1012.
(70) Saraji-Bozorgzad, M.; Geissier, R.; Streibel, T.; Muhlberger, F.; Sklorz, M.; Kaisersberger, E.; Denner, T.; Zimmermann, R. Thermogravimetry coupled to single photon ionization quadrupole mass spectrometry: A tool to investigate the chemical signature of thermal decomposition of polymeric materials. *Anal. Chem.* **2008**, *80*, 3393−3403.
(71) Dorfner, R.; Ferge, T.; Yeretzian, C.; Kettrup, A.; Zimmermann, R. Laser mass spectrometry as on-line sensor for industrial process analysis: Process control of coffee roasting. *Anal. Chem.* **2004**, *76*, 1386−1402.
(72) Muhlberger, F.; Streibel, T.; Weiser, J.; Ulrich, A.; Zimmermann, R. Single photon ionization time-of-flight mass spectrometry with a pulsed electron beam pumped excimer VUV lamp for on-line gas analysis: Setup and first results on cigarette smoke and human breath. *Anal. Chem.* **2005**, *77*, 7408−7414.
(73) Finch, J. W.; Toerne, K. A.; Schram, K. H.; Denton, M. B. Evaluation of a hydrogen laser vacuum ultraviolet source for photoionization mass spectrometry of pharmaceuticals. *Rapid Commun. Mass Spectrom.* **2005**, *19*, 15−22.
(74) Becker, C. H.; Wu, K. J. On the photoionization of large molecules. *J. Am. Soc. Mass Spectrom.* **1995**, *6*, 883−888.
(75) Marksteiner, M.; Haslinger, P.; Ulbricht, H.; Sclafani, M.; Oberhofer, H.; Dellago, C.; Arndt, M. Gas-phase formation of large neutral alkaline-earth metal tryptophan complexes. *J. Am. Soc. Mass Spectrom.* **2008**, *19*, 1021−1026.
(76) Belau, L.; Wilson, K. R.; Leone, S. R.; Ahmed, M. Vacuum-ultraviolet photoionization studies of the microhydration of DNA bases (guanine, cytosine, adenine, and thymine). *J. Phys. Chem. A* **2007**, *111*, 7562−7568.
(77) Heinbuch, S.; Dong, F.; Rocca, J. J.; Bernstein, E. R. Single photon ionization of van der Waals clusters with a soft X-ray laser: $(CO_2)_n$ and $(CO_2)_n(H_2O)_m$. *J. Chem. Phys.* **2006**, *125*, 154316.
(78) Heinbuch, S.; Dong, F.; Rocca, J. J.; Bernstein, E. R. Single photon ionization of hydrogen bonded clusters with a soft X-ray laser: $(HCOOH)_x$ and $(HCOOH)_y(H_2O)_z$. *J. Chem. Phys.* **2007**, *126*, 244301.
(79) Andrews, A. B.; Edwards, J. C.; Pomerantz, A. E.; Mullins, O. C.; Nordlund, D.; Norinaga, K. Comparison of coal-derived and petroleum asphaltenes by ^{13}C nuclear magnetic resonance, DEPT, and XRS. *Energy Fuels* **2011**, *25*, 3068−3076.
(80) Ruiz-Morales, Y.; Mullins, O. C. Polycyclic aromatic hydrocarbons of asphaltenes analyzed by molecular orbital calculations with optical spectroscopy. *Energy Fuels* **2007**, *21*, 256−265.
(81) Park, J.; Qin, H.; Scalf, M.; Hilger, R. T.; Westphall, M. S.; Smith, L. M.; Blick, R. H. A mechanical nanomembrane detector for time-of-flight mass spectrometry. *Nano Lett.* **2011**, *11*, 3681−3684.
(82) Dehareng, D.; Dive, G. Vertical ionization energies of α-L-amino acids as a function of their conformation: An *ab initio* study. *Int. J. Mol. Sci.* **2004**, *5*, 301−332.
(83) Hoelz, L. V. B.; Horta, B. A. C.; Araújo, J. Q.; Albuquerque, M. G.; de Alencastro, R. B.; da Silva, J. F. M. Quantitative structure−activity relationships of antioxidant phenolic compounds. *J. Chem. Pharm. Res.* **2010**, *2*, 291−306.
(84) Hammond, M. R.; Zare, R. N. Identifying the source of a strong fullerene envelope arising from laser desorption mass spectrometric analysis of meteoritic insoluble organic matter. *Geochim. Cosmochim. Acta* **2008**, *72*, 5521−5529.

DOI: 10.1021/ef5020764
Energy Fuels 2015, 29, 2833−2842

(85) Rodgers, R. P.; Hendrickson, C. L.; Emmett, M. R.; Marshall, A. G.; Greaney, M.; Qian, K. Molecular characterization of petroporphyrins in crude oil by electrospray ionization Fourier transform ion cyclotron resonance mass spectrometry. *Can. J. Chem.* **2001**, *79*, 546−551.
(86) Qian, K.; Rodgers, R. P.; Hendrickson, C. L.; Emmett, M. R.; Marshall, A. G. Reading chemical fine print: Resolution and identification of 3000 nitrogen-containing aromatic compounds from a single electrospray ionization Fourier transform ion cyclotron resonance mass spectrum of heavy petroleum crude oil. *Energy Fuels* **2001**, *15*, 492−498.
(87) Gemechu, A. S.; Hoffmann, L. J. H.; Marquardt, S.; Eisenhardt, C. G.; Baumgärtel, H.; Chelli, R.; Cardini, G.; Califano, S. The absorption spectrum of anisole and the anisole/CO_2 1:1-cluster. The influence of intermolecular interaction and intramolecular vibrations. *Z. Phys. Chem.* **2004**, *218*, 123−153.
(88) Buenrostro-Gonzalez, E.; Groenzin, H.; Lira-Galeana, C.; Mullins, O. C. The overriding chemical principles that define asphaltenes. *Energy Fuels* **2001**, *15*, 972−978.
(89) Goual, L.; Sedghi, M.; Mostowfi, F.; McFarlane, R.; Pomerantz, A. E.; Saraji, S.; Mullins, O. C. Cluster of asphaltene nanoaggregates by DC conductivity and centrifugation. *Energy Fuels* **2014**, *28*, 5002−5013.
(90) Zhan, D.; Fenn, J. B. Electrospray mass spectrometry of fossil fuels. *Int. J. Mass Spectrom.* **2000**, *194*, 197−208.
(91) Stabel, A.; Herwig, P.; Müllen, K.; Rabe, J. P. Diodelike current−voltage curves for a single molecule—Tunneling spectroscopy with submolecular resolution of an alkylated, peri-condensed hexabenzocoronene. *Angew. Chem., Int. Ed.* **1995**, *34*, 1609−1611.
(92) Lisitza, N. V.; Freed, D. E.; Sen, P. N.; Song, Y.-Q. Study of asphaltene nanoaggregation by nuclear magnetic resonance (NMR). *Energy Fuels* **2009**, *23*, 1189−1193.
(93) Andreatta, G.; Bostrom, N.; Mullins, O. C. High-*Q* ultrasonic determination of the critical nanoaggregate concentration of asphaltenes and the critical micelle concentration of standard surfactants. *Langmuir* **2005**, *21*, 2728−2736.
(94) Pomerantz, A. E.; Seifert, D. J.; Bake, K. D.; Craddock, P. R.; Mullins, O. C.; Kodalen, B. G.; Mitra-Kirtley, S.; Bolin, T. B. Sulfur chemistry of asphaltenes from a highly compositionally graded oil column. *Energy Fuels* **2013**, *27*, 4604−4608.
(95) Dutta Majumdar, R.; Gerken, M.; Mikula, R.; Hazendonk, P. Validation of the Yen−Mullins model of Athabasca oil-sands asphaltenes using solution-state ^{1}H NMR relaxation and 2D HSQC spectroscopy. *Energy Fuels* **2013**, *27*, 6528−6537.
(96) Korb, J. P.; Louis-Joseph, A.; Benamsili, L. Probing structure and dynamics of bulk and confined crude oils by multiscale NMR spectroscopy, diffusometry, and relaxometry. *J. Phys. Chem. B* **2013**, *117*, 7002−7014.
(97) Rane, J. P.; Pauchard, V.; Couzis, A.; Banerjee, S. Interfacial rheology of asphaltenes at oil−water interfaces and interpretation of the equation of state. *Langmuir* **2013**, *29*, 4750−4759.
(98) Rane, J. P.; Harbottle, D.; Pauchard, V.; Couzis, A.; Banerjee, S. Adsorption kinetics of asphaltenes at the oil−water interface and nanoaggregation in the bulk. *Langmuir* **2012**, *28*, 9986−9995.
(99) Eyssautier, J.; Levitz, P.; Espinat, D.; Jestin, J.; Gummel, J.; Grillo, I.; Barre, L. Insight into asphaltene nanoaggregate structure inferred by small angle neutron and X-ray scattering. *J. Phys. Chem. B* **2011**, *115*, 6827−6837.

DOI: 10.1021/ef5020764
Energy Fuels 2015, 29, 2833−2842